Physical interpretation on eigen-parameters of polarimetric SAR data for microwave scattering from leaf

Sang-Eun Park
School of Earth & Environmental Science (SEES), Kwan-ak Gu Shil-rim dong san 56-1, Seoul National University, Seoul 151-742, Korea (separk@eos1.snu.ac.kr)

Wooil M. Moon [1, 2]
1. School of Earth & Environmental Sciences (SEES), Kwan-ak Gu Shil-rim dong san 56-1, Seoul National University, Seoul 151-742, Korea (wmoon@eos1.snu.ac.kr)
2. Geophysics, University of Manitoba, Winnipeg, MB R3T 2N2 Canada (wmoon@cc.umanitoba.ca)

Abstract: An eigen-analysis of the coherency matrix provides the polarimetric scattering mechanisms with the matrix characterizing parameters. In this paper, the coherency matrices of deciduous and coniferous vegetation are calculated using the analytical method. The Generalized Rayleigh-Gans approximation is used to model backscattering from distributed coniferous and deciduous leaves. The characteristics of eigen-parameters of simulated coherency matrix for deciduous and coniferous leaves with respect to the leaf shapes and orientations are illustrated.

1. Introduction

A major problem in analyzing polarimetric SAR data is in understanding the scattering mechanisms. An eigen-analysis of the coherency matrix provides the scattering information with the matrix characterizing parameters such as the polarimetric Entropy *H*, the polarimetric Anisotropy *A*, and the mean polarimetric scattering angles. Eigen-parameters have been widely used for modeling and classification of Polarimetric SAR data [1-4]. However, eigen-parameters are not physically based, and the interpretation of results is not unique especially for the multiple and/or volume scattering problems in vegetated terrain. In general, leaves constitute a major part of a vegetation canopy. In this paper, the characteristics of eigen-parameters obtained from the analytic coherency matrix of deciduous and coniferous leaves are investigated. The Generalized Rayleigh-Gans (GRG) approximation is used to model backscattering from distributed elliptic- and needle-shaped deciduous and coniferous leaves, respectively. In addition, the differences between the eigen-parameters of the elliptic and needle leaves are illustrated numerically for different orientation and incidence angles.

2. Eigen-analysis of Coherency Matrix

The polarimetric backscattering problem can be described in feature vector with Pauli basis set such as

$$\vec{k}_P = \frac{1}{\sqrt{2}}\left[S_{HH} + S_{VV} \quad S_{HH} - S_{VV} \quad 2S_{HV}\right]^T, \quad (1)$$

For incoherent scattering cases, received wave is the vector sum of the waves scattered from all the individual scattering centers. Statistically fluctuated scatterers are completely described by the coherency matrix $[T]$ defined as

$$[T] = \left\langle \vec{k}_P \cdot \vec{k}_P^{+} \right\rangle \quad (2)$$

where <…> denotes a spatial ensemble averaging, and + denote the complex conjugate transpose. The coherency matrix is by definition a hermitian matrix, which can be decomposed into a real eigenvalue spectrum and orthogonal unitary eigenvectors [5];

$$[T] = [U_3][\Sigma][U_3]^{-1} = \sum_{i=1}^{3} \lambda_i \hat{\mathrm{u}}_i \cdot \hat{\mathrm{u}}_i^{+} \quad (3)$$

where $[\Sigma]$ is a 3×3 diagonal matrix with real eigenvalues and $[U_3] = [\hat{u}_1 \quad \hat{u}_2 \quad \hat{u}_3]$ is a unitary matrix with the three orthogonal eigenvectors. The polarimetric Entropy *H* is defined in terms of the logarithmic sum of eigenvalues as

$$H = -\sum_{i=1}^{3} P_i \log_3(P_i) \quad P_i = \lambda_i \left(\sum_{j=1}^{3} \lambda_j \right)^{-1} \quad (4)$$

While the polarimetric Entropy is a useful scalar descriptor of the randomness of the scattering process, another eigenvalue parameter defined as the Anisotropy A_n can be introduced;

$$A_n = \frac{\lambda_2 - \lambda_3}{\lambda_2 + \lambda_3}. \quad (5)$$

Anisotropy indicates the presence of multiple scattering.

The parameterization of the eigenvectors have been introduced [5] as

$$\hat{\mathrm{u}}_i = \left[\cos\alpha_i \quad \sin\alpha_i \cos\beta_i e^{(j\delta_i)} \quad \sin\alpha_i \sin\beta_i e^{(j\gamma_i)}\right]^T. \quad (6)$$

The polarimetric target can be modeled as sums of the parameterization of $[U_3]$ in Eq.(3), which occur with probabilities P_i. The mean α angle may then be defined as

$$\bar{\alpha} = \sum_{i=1}^{3} P_i \alpha_i = P_1\alpha_1 + P_2\alpha_2 + P_3\alpha_3. \quad (7)$$

In general, $\bar{\alpha}$ reveals the averaged scattering mechanisms ranging surface scattering to double bounce scattering.

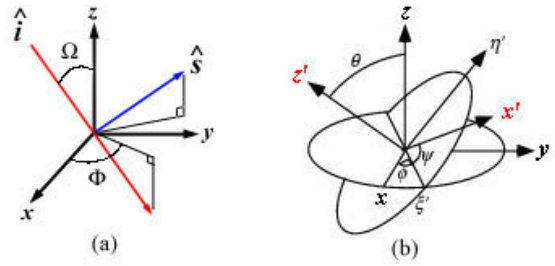

Fig. 1. (a) Global scattering coordinate system configuration for leaf scattering model, and (b) Eulerian angle of orientation.

3. Leaf Scattering Model

Scattering from randomly oriented dielectric non-spherical scatters with shape and dielectric constant similar to the vegetation components has been used to model electromagnetic wave scattering from leaves [6,7]. In the microwave frequency region where the leaf dimensions are of the order of the incident wavelength, the GRG approximation is needed to model the scattering amplitude from leaves. In this study, randomly oriented identical elliptic disks are used to model leaves in deciduous vegetation, and randomly oriented identical needles in coniferous vegetation. For the GRG approach, the full scattering amplitude tensor is given by

$$\overline{\overline{S}}(\hat{s},\hat{i}) = \frac{k^2(\varepsilon_r - 1)v_0}{4\pi}\left(\overline{\overline{I}} - \hat{s}\hat{s}\right)\cdot\overline{\overline{a}}\cdot\left(\overline{\overline{I}} - \hat{i}\hat{i}\right)\mu(\hat{s},\hat{i}) \quad (8)$$

where k is the free space wave number, ε_r is the leaf relative dielectric constant, v_0 is the leaf volume, $\overline{\overline{a}}$ is the polarizability tensor [7], $\mu(\hat{s},\hat{i})$ is the modifying function to the Rayleigh scattering [8], and $\hat{i}$, $\hat{s}$ represent the incident and scattered direction, respectively (Fig.1).

Spatial ensemble average <…> is taken over the leaf orientation as

$$\left\langle \left|S_{pq}\right|^2 \right\rangle = \iiint p(\phi)p(\theta)p(\psi)\left|S_{pq}\right|^2 d\phi\, d\theta\, d\psi \quad (9)$$

where (ϕ,θ,ψ) are the leaf-orientation angles defined as Eulerian angles with respect to the reference frame as shown in Fig.1(b), and $p(\phi), p(\theta), p(\psi)$ are the probability distribution function of the leaf orientations. To simulate a medium of randomly distributed leaves with some preferred orientations with respect to the reference frame, the angle ϕ is assumed to be uniformly distributed in the azimuth $(p(\phi) = 1/2\pi)$, while the distribution for θ and ψ can be chosen as follows:

$$p(X) = \begin{cases} \dfrac{1}{X_2 - X_1}, X_1 < X < X_1 \\ 0, \quad \text{otherwise} \end{cases} \quad (10)$$

where $X = \theta$ or ψ . Different values of $\Delta\theta$ and $\Delta\psi$ are used to describe leaf orientation effect on radar backscatter.

4. Simulation Results

The coherency matrix of elliptic disks and needles are calculated using GRG approximation. The simulation is performed at a frequency of 1.24 GHz. The leaf dielectric constant is assumed to equal $19.54 - j5.54$. The Entropy and averaged alpha values as a function of incidence angles and leaf-orientation angles are shown in Fig.2 and Fig.3. The leaf parameters are: the semi-major axis 5 cm, the semi- minor axis 1.25 cm, and the thickness 0.1 mm for the elliptic disk. The radius of needle is assumed to be 0.12 cm, and its height is assumed to be 5 cm. In the Eulerian angle of leaf-orientation, θ are used to denote the normal of the disk scatter or the orientation of the needle axis. When the elliptic and needle leaves are nearly horizontal, i.e. small $\Delta\theta$, the shape of leaves can not be separable in $H/\overline{\alpha}$ plane, and $\overline{\alpha}$ increase with respect to

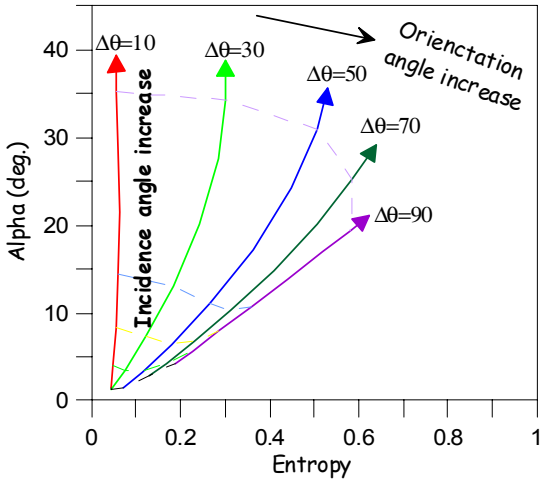

Fig. 2. The Entropy and $\overline{\alpha}$ values for the elliptic Disks.

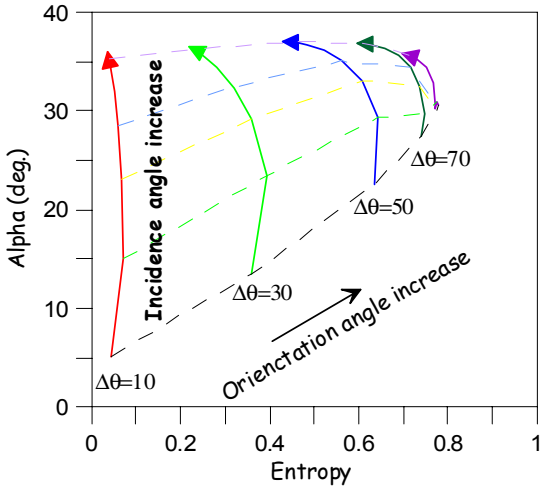

Fig. 3. The Entropy and $\overline{\alpha}$ values for the needle leaves.

the incidence angle. At a given incidence angle, $\overline{\alpha}$ decreases for elliptic leaves as the distribution ranges of orientation angle increase, while it increases for needle leaves. In this case, we can differentiate types of the leaf shape using $\overline{\alpha}$ values. When leaves are identical in size, the $\overline{\alpha}$ value is highly connected to the variation of the incidence angle which is related to the changes in scattering mechanism.

Fig. 4 shows differences between two eigenvalue parameters in Eq. (4-5) as a function of incidence angles.

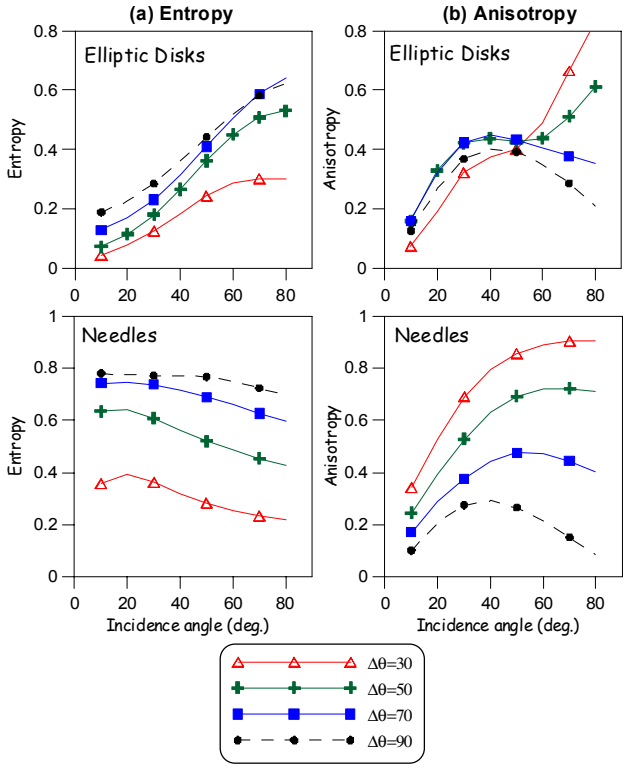

Fig. 4. (a) The Entropy and (b) the Anisotropy values versus the incidence angle for the elliptic disk (upper law) and needle leave (lower law).

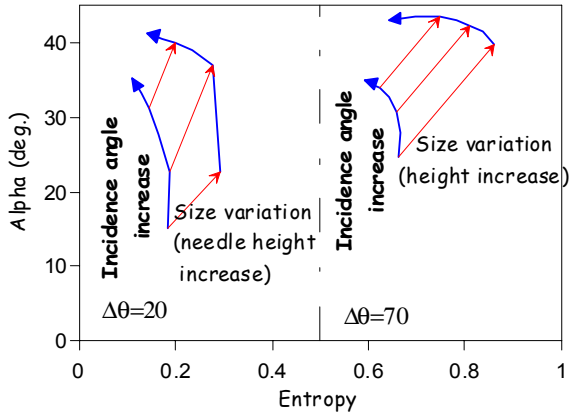

Fig. 5. The Entropy and $\overline{\alpha}$ values as a function of incidence angles and leaf size variation for needle

Anisotropy values are more sensitive to the variation of incidence angle. Anisotropy can be a strong indicator of the distribution ranges of orientation angle especially for the high incidence angle region.

We also examined the effect of size variation on eigen-parameters. The Entropy and $\overline{\alpha}$ values as a function of incidence angles and leaf size variation for needle leaves are shown in Fig. 5. Entropy and $\overline{\alpha}$ values increase with respect to the height of the needle leaves. Following simulated results in Fig. 3 and Fig. 5, $\overline{\alpha}$ values are more affected by the size variation than leaf-orientation angles.

4. Conclusions

The physical information and their relations of eigen-parameters are studied using simulated coherency matrix from disk- and needle-shaped deciduous and coniferous leaves, respectively. When leaves are identical in size, the $\overline{\alpha}$ value is highly connected to the variation of the incidence angle which is related to the changes in scattering mechanism. Entropy values are related to the distribution of leaf-orientation. Anisotropy can be a better indicator of the distribution ranges of orientation angle than entropy especially for the high incidence angle region. $\overline{\alpha}$ values are more affected by the size variation than leaf-orientation angles.

Acknowledgment

This research is funded by the SEES (BK21), Seoul National University, and NSERC of Canada grant (A-7400) to W. M. Moon.

References

[1] Cloude S. R., and Pottier E., 1997. An Entropy based classification scheme for land applications of polarimetric SAR, *IEEE Trans. Geosci. Remote Sensing*, Vol. 35, pp. 68-78.

[2] Wang Y., and Davis F. W., 1997. Decomposition of polarimetric synthetic aperture radar backscatter from upland and flooded forests, *Int. J. Remote Sensing*, vol. 18, No. 6, pp. 1319-1332.

[3] Ferro-Famil L., Pottier E. and Lee J. S., 2001. Unsupervised classification of multifrequency and fully polarimetric SAR images based on the H/A Alpha - Wishart classifier, *IEEE Trans. Geosci. Remote Sensing*, Vol. 39, No 11, pp. 2332 – 2342.

[4] Cloude S. R., and D. G Corr, 2002. A New Parameter for Soil Moisture Estimation, P*roc. IGARSS 2002*,Toronto, pp 641-643.

[5] Cloude S. R., and Pottier E., 1996. A review of target decomposition theorems in radar polarimetry, *IEEE Trans. Geosci. Remote Sensing*, Vol. 34, pp. 498-518.

[6] Karam M. A., and Fung A. K., 1989. Leaf-Shape Effects in Electromagnetic Wave Scattering From Vegetation, *IEEE Trans. Geosci. Remote Sensing*, Vol. 27, no. 6, pp. 687-697.

[7] Van de Hulst H. C., 1981. *Light Scattering by Small Particles*, New York, Dover, pp. 63-73.

[8] Karam M. A., Fung A. K., and Antar Y., 1988. Electromagnetic Wave Scattering from Some Vegetation Samples, *IEEE Trans. Geosci. Remote Sensing*, Vol. 26, no. 6, pp. 799-808.